

Disordered contacts can localize helical edge electrons

Arjun Mani and Colin Benjamin*

School of Physical Sciences, National Institute of Science Education & Research, HBNI, Jatni-752050, India

It is well known that quantum spin Hall (QSH) edge modes being helical are immune to backscattering due to non-magnetic disorder within the sample. Thus, quantum spin Hall edge modes are non-localized and show a vanishing Hall resistance along with quantized 2-terminal, longitudinal and non-local resistances even in presence of sample disorder. However, this is not the case for contact disorder. This paper shows that when all contacts are disordered in a N-terminal quantum spin Hall sample, then transport via these helical QSH edge modes can have a significant localization correction. All the resistances in a N-terminal quantum spin Hall sample deviate from their values derived while neglecting the phase acquired at disordered contacts, and this deviation is called the quantum localization correction. This correction term increases with the increase of disorderedness of contacts but decreases with the increase in number of contacts in a N terminal sample. The presence of inelastic scattering, however, can completely destroy the quantum localization correction.

I. INTRODUCTION

The quantum spin Hall effect observed in a 2D topological insulator is known for transport via dissipation-less helical 1D edge modes. These 1D helical edge modes are robust to sample disorder and are observed in systems like HgTe/CdTe heterostructures at low temperatures, due to bulk spin orbit effects and in absence of a magnetic field [1–3]. QSH edge modes are helical, i.e., at the upper edge a spin-up electron moves in one direction while spin-down electron moves in opposite direction while at the lower edge the directions are reversed, see Fig. 1. Thus, quantum spin Hall systems are invariant under time reversal symmetry. Due to the topological nature of these edge modes, the Hall resistance vanishes, while the 2-terminal, longitudinal and non-local resistances are quantized at $\frac{3}{2} \frac{h}{2e^2}$, $\frac{1}{2} \frac{h}{2e^2}$ and $\frac{1}{6} \frac{h}{2e^2}$ respectively in a six terminal ideal QSH sample (without any disordered contacts). The Hall, longitudinal, 2-terminal and non-local conductances/resistances are determined by resorting to the Landauer-Buttiker(L-B) theory[5, 6]. In this formalism, for a QSH device with N contacts, the current at contact i at zero temperature is[5–7]:

$$I_i = \frac{e^2}{h} \sum_{j=1, j \neq i}^N \sum_{\sigma, \sigma'} [T_{ji}^{\sigma\sigma'} V_i - T_{ij}^{\sigma\sigma'} V_j], \text{ with } T_{ij}^{\sigma\sigma'} = \text{Tr}[s_{ij}^{\sigma\sigma'} \dagger s_{ij}^{\sigma\sigma'}], \quad (1)$$

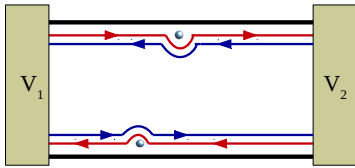


Figure 1. Helical QSH edge modes are immune to sample disorder.

where $T_{ij}^{\sigma\sigma'}$ is the transmission probability for an electronic edge mode from contact j to contact i with initial spin σ' to final

spin σ , V_i being the voltage bias applied at contact i , while $s_{ij}^{\sigma\sigma'}$ are the elements of the scattering matrix S of the N -terminal sample.

II. MOTIVATION

In quantum diffusive transport regime, localization of electronic states is well known [4, 5], the resistance of a sample increases exponentially with sample length (l) for $l > \xi$ (ξ being localization length) [5]. This is known as strong or Anderson localization[12, 13]. On the other hand, when the sample length $l \leq \xi$, the system shows a unique property: the resistance increases from the Ohmic result by universal factor $h/2e^2$. This increase by the universal factor $h/2e^2$ is called as weak localization correction. The QSH edge modes, as shown in Fig. 1, are immune to backscattering, e.g., if there is disorder in the sample (see, Fig. 1), edge modes will move around the disorder without their transmission probabilities getting affected due to topological protection. In this work we however predict that, if a contact is disordered, i.e., can reflect edge modes partially then a “quantum” localization correction can arise for edge modes too but only when all contacts are disordered. What happens is backscattering of the electrons within the sample takes place when all contacts are disordered and thus multiple paths are generated from one contact to another. As a result, the transmission probabilities and resistances become dependent on the disorderedness of contacts. However, it should be noted that this quantum localization observed for QSH edge modes is different from the weak localization correction seen in context of quantum diffusive transport. In quantum diffusive transport regime, the weak localization correction is universal ($h/2e^2$), while in our case, the correction due to localization as will be discussed in more detail in sections III and IV, depends on the strength of disorder at contacts and on the number of contacts. Further, this quantum localization correction is present only when all contacts are disordered, see Fig. 2(a). In Fig. 2(a), a_i^σ and b_i^σ refer to the incoming and outgoing edge states respectively from sample to contact i with σ being the spin index for that edge state. In Fig. 2(a), we see that a spin up electron in the a_1^\uparrow edge state at contact 1 can either transmit into the sample with

* colin.nano@gmail.com

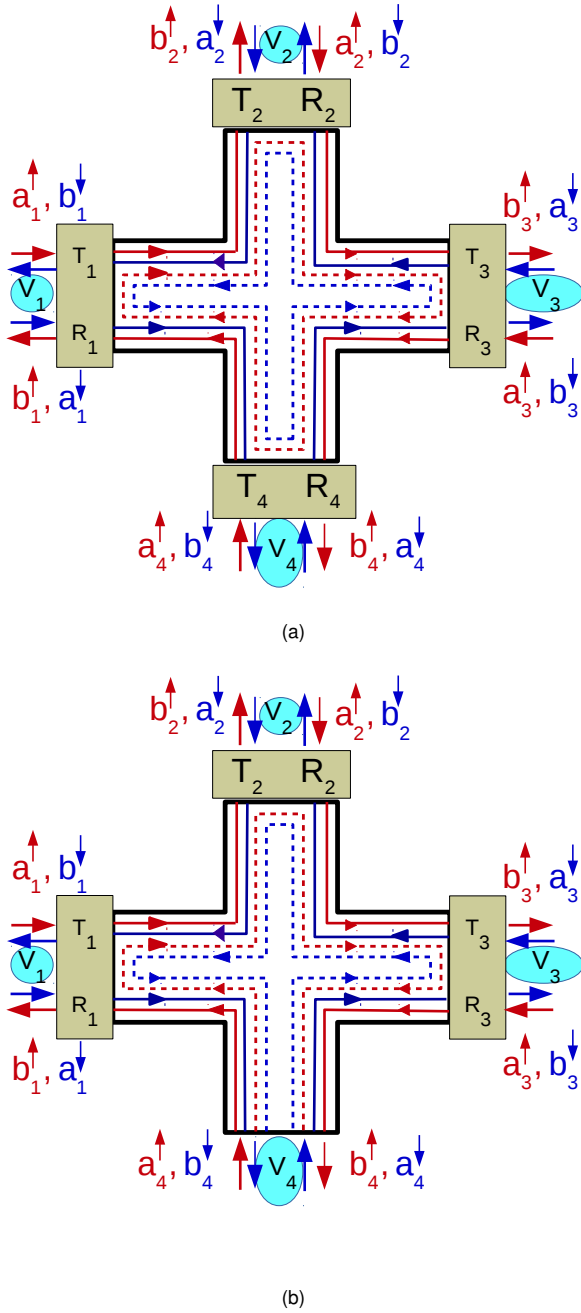


Figure 2. (a) Pictorial representation to explain the origin of quantum localization correction when all contacts are disordered in a 4T QSH sample. (b) Absence of quantum localization correction in a 4T QSH sample when only 3 of the 4 contacts are disordered.

probability T_1 or reflect back again to contact 1 with probability R_1 . After entering the sample, this edge state electron can reach contact 3 via reflection at contact 2 with probability R_2 and then transmit to contact 3 with probability T_3 . Thus the transmission probability for a spin-up edge electron from contact 1 to 3 is $T_1 R_2 T_3$. This is one among the infinite number of paths possible. For example, it can also reach contact 3 by taking second path after reflecting at contacts 3, 4, 1, 2 and then finally transmitting into contact 3 with transmission

probability $T_1 T_3 R_1 R_2^2 R_3 R_4$. Thus, summing all paths from contact 1 to 3, we get the net transmission probability for the spin up edge state- $T_{31}^{\uparrow\uparrow} = T_1 R_2 T_3 / (1 - R_1 R_2 R_3 R_4)$. However, by taking recourse to scattering amplitudes instead of probabilities we get the transmission amplitude from contact 1 to 3 as $t_{31}^{\uparrow\uparrow} = -t_1 r_2 t_3 e^{i(\phi - \phi_4)} / (1 - r_1 r_2 r_3 r_4 e^{i\phi})$, where t_i and r_i are the transmission and reflection amplitudes at contact i with ϕ_i being the phase acquired by the electron at contact i and $\phi = \sum_i \phi_i$. This scattering amplitude will lead to the transmission probability from contact 1 to 3 for spin up edge state- $T_{31}^{\uparrow\uparrow} = |t_{31}^{\uparrow\uparrow}|^2 = T_1 R_2 T_3 / (1 + R_1 R_2 R_3 R_4 - 2\sqrt{R_1 R_2 R_3 R_4} \cos \phi)$. This is different to what was derived earlier for $T_{31}^{\uparrow\uparrow}$. Similarly, rest of the transmission probabilities can be calculated by considering transmission probabilities or via following scattering amplitudes, and these too will be different for each case. Thus, when an infinite number of paths exist from one contact to another then a difference between the average resistances derived from scattering amplitudes $\langle R_X^{Amp} \rangle$ (wherein $X = H, L, 2T, NL$ denotes Hall, Longitudinal, Two-terminal and Non-local) and resistances derived from probabilities R_X , i.e., $\langle R_X^{Amp} \rangle \neq R_X$ is seen. This situation changes, if however at least one of the contacts is not disordered, see Fig. 2(b) (wherein contact 4 is not disordered), in this case there are a finite number of paths from one contact to another. This can be seen as follows: in Fig. 2(b), a spin up edge state from contact 1 can reach contact 3 by following only one path via reflection at contact 2 with probability $T_{31}^{\uparrow\uparrow} = T_1 R_2 T_3$. There is no second path to reach contact 3, since contact 4 is not disordered, this edge state can not reflect from contact 4. Further, the scattering amplitude from contact 1 to 3 is $t_{31}^{\uparrow\uparrow} = -t_1 r_2 t_3 e^{i(\phi - \phi_4)}$, which gives the transmission probability $T_{31}^{\uparrow\uparrow} = |t_{31}^{\uparrow\uparrow}|^2 = T_1 R_2 T_3$. Thus the calculation using scattering probabilities and that with scattering amplitudes yield identical results for the case when less than N contacts are disordered. This results in $\langle R_X^{Amp} \rangle = R_X$ for the case when less than N contacts are disordered and thus quantum localization correction vanishes. Similar, to what is described here for QSH system, was also shown recently for quantum Hall (QH) system in Ref. [9]. This is the main motivation of our work, can we see a similar quantum localization correction for QSH samples? Since QSH edge modes are helical (spin polarized) rather than chiral (spin unpolarized) as in QH sample, it will be interesting to see the effect of spin polarized and helical edge modes on the quantum localization correction. Further, to compare the characteristics of this quantum localization correction in various resistances for both QH and QSH systems is another motivation of this paper. We elaborate on this in sections III, IV and V for four, six and N-terminal QSH samples respectively. The topic of research undertaken in this paper is both timely as well as novel. Since understanding why in quantum spin Hall experiments the robust quantized conductance is absent is a hotly debated topic of research. Reasons for the less than robust quantization of spin Hall conduction have ranged from magnetic impurities to inelastic scattering as well as to hyperfine interaction which will break time reversal symmetry and therefore induce backscattering of edge modes[10]. In this manuscript, we show that even when either there is no inelas-

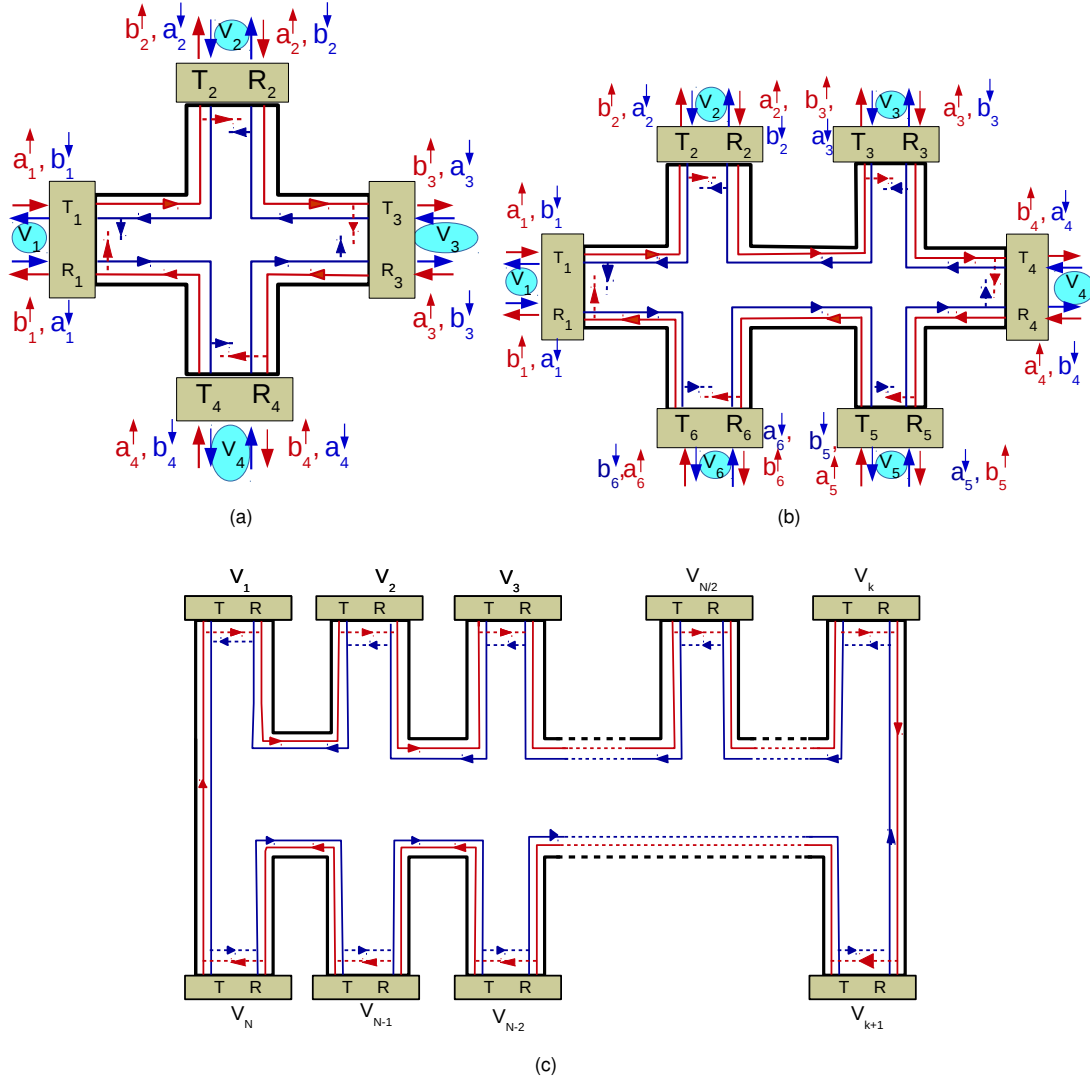


Figure 3. (a) 4-terminal, (b) 6-terminal and (c) N-terminal QSH sample with all disordered contacts.

tic scattering or in absence of magnetic impurities or even for no hyperfine interaction[11] there still can be loss in quantized conductance which we call a quantum localization correction due to disordered contacts alone. Further all the proposals to explain the loss of quantization of helical conduction in quantum spin Hall samples rely on some kind of inelastic scattering which is dealt with via many body interactions. Our paper is novel in that we via a single particle theory explain the loss of quantized conduction which we dub the quantum localization correction to helical edge transport.

The organization of this paper is as follows: in section III, we deal with a 4-terminal QSH sample with all disordered contacts and derive an expression for the quantum localization correction, while in sections IV and V we discuss the six and N-terminal QSH samples. Next in section VI, we study the impact of inelastic scattering on this quantum localization correction. We conclude with a table summarizing the main results of our paper and compare it with results derived in Ref. [9].

III. FOUR TERMINAL SYSTEM WITH ALL DISORDERED CONTACTS

A 4-terminal QSH sample is shown in Fig. 3(a) with all disordered contacts. The strength of disorder at contact i is defined by D_i and it is related to the reflection (R_i) and transmission probabilities (T_i) of an edge state at contact i by the relation $D_i = R_i = 1 - T_i$. Contacts 1, 3 are current probes while contacts 2, 4 are voltage probes, such that $I_2 = I_4 = 0$. For calculating the current at each of these contacts, we need to derive the edge state transmission probability $T_{ij}^{\sigma\sigma'}$ between these contacts. Since all contacts are disordered, we need to consider the scattering amplitudes to calculate the transmission probabilities $T_{ij}^{\sigma\sigma'}$, from Eq. (1). First we write down the scattering matrix S_j at each contact j separately relating incoming edge modes ($a_j^\uparrow, a_j^\downarrow, a_j^\uparrow, a_j^\downarrow$) to outgoing edge modes ($b_j^\uparrow, b_j^\downarrow, b_j^\uparrow, b_j^\downarrow$) at that particular contact j and then deduce the full scattering matrix S of the system out of the contact scattering matrices S_j , see Ref. [18]. The scattering matrix S_j is

defined as follows

$$S_j = \begin{pmatrix} r_j e^{i\phi_j^{\uparrow\uparrow}} & 0 & t_j e^{i\phi_j^{\uparrow\downarrow}} & 0 \\ 0 & r_j e^{i\phi_j^{\downarrow\downarrow}} & 0 & t_j e^{i\phi_j^{\downarrow\uparrow}} \\ t_j e^{i\phi_j^{\downarrow\uparrow}} & 0 & r_j e^{i\phi_j^{\downarrow\downarrow}} & 0 \\ 0 & t_j e^{i\phi_j^{\downarrow\uparrow}} & 0 & r_j e^{i\phi_j^{\downarrow\downarrow}} \end{pmatrix}, \quad (2)$$

where r_j and t_j are the reflection and transmission amplitudes respectively at contact j , $\phi_j^{\uparrow\sigma}$ and $\phi_j^{\downarrow\sigma}$ are the reflection and transmission phase acquired by the spin σ ($=\uparrow/\downarrow$) edge electron via scattering at the disordered contact j . Unitarity of the scattering matrix S_j dictates $S_j^\dagger S_j = S_j S_j^\dagger = \mathbb{1}$, which implies $\phi_j^{\uparrow\sigma} = \phi_j^{\downarrow\sigma} - \frac{\pi}{2} = \phi_j$, (dropping the spin index σ from the phase as disorder is spin independent). Thus the scattering matrix S_j reduces to

$$S_j = \begin{pmatrix} r_j e^{i\phi_j} & 0 & it_j e^{i\phi_j} & 0 \\ 0 & r_j e^{i\phi_j} & 0 & it_j e^{i\phi_j} \\ it_j e^{i\phi_j} & 0 & r_j e^{i\phi_j} & 0 \\ 0 & it_j e^{i\phi_j} & 0 & r_j e^{i\phi_j} \end{pmatrix}. \quad (3)$$

$$S = \frac{1}{a} \begin{pmatrix} (r_1 - r_2 r_3 r_4 e^{i\phi}) e^{i\phi_1} & 0 & -t_1 t_2 r_3 r_4 e^{i\phi} & 0 & -t_1 t_3 r_4 e^{i(\phi - \phi_2)} & 0 & -t_1 t_4 e^{i(\phi_1 + \phi_4)} & 0 \\ 0 & (r_1 - r_2 r_3 r_4 e^{i\phi}) e^{i\phi_1} & 0 & -t_1 t_2 e^{i(\phi_1 + \phi_2)} & 0 & -t_1 t_3 r_2 e^{i(\phi - \phi_4)} & 0 & -t_1 t_4 r_2 r_3 e^{i\phi} \\ -t_1 t_2 e^{i(\phi_1 + \phi_2)} & 0 & (r_2 - r_1 r_3 r_4 e^{i\phi}) e^{i\phi_2} & 0 & -t_2 t_3 r_1 r_4 e^{i\phi} & 0 & -t_2 t_4 r_1 e^{i(\phi - \phi_3)} & 0 \\ 0 & -t_1 t_2 r_3 r_4 e^{i\phi} & 0 & (r_2 - r_1 r_3 r_4 e^{i\phi}) e^{i\phi_2} & 0 & -t_2 t_3 e^{i(\phi_2 + \phi_3)} & 0 & -t_2 t_4 r_3 e^{i(\phi - \phi_1)} \\ -t_1 t_3 r_2 e^{i(\phi - \phi_4)} & 0 & -t_2 t_3 e^{i(\phi_2 + \phi_3)} & 0 & (r_3 - r_1 r_2 r_4 e^{i\phi}) e^{i\phi_3} & 0 & -t_3 t_4 r_1 r_2 e^{i\phi} & 0 \\ 0 & -t_1 t_3 r_4 e^{i(\phi - \phi_2)} & 0 & -t_2 t_3 r_1 r_4 e^{i\phi} & 0 & (r_3 - r_1 r_2 r_4 e^{i\phi}) e^{i\phi_3} & 0 & -t_3 t_4 e^{i(\phi_3 + \phi_4)} \\ -t_1 t_4 r_3 r_2 e^{i\phi} & 0 & -t_2 t_4 r_3 e^{i(\phi - \phi_1)} & 0 & -t_3 t_4 e^{i(\phi_3 + \phi_4)} & 0 & (r_4 - r_1 r_2 r_3 e^{i\phi}) e^{i\phi_4} & 0 \\ 0 & -t_1 t_4 e^{i(\phi_1 + \phi_4)} & 0 & -t_2 t_4 r_1 e^{i(\phi - \phi_3)} & 0 & -t_3 t_4 r_1 r_2 e^{i\phi} & 0 & (r_4 - r_1 r_2 r_3 e^{i\phi}) e^{i\phi_4} \end{pmatrix}, \quad (4)$$

where $a = 1 - r_1 r_2 r_3 r_4 e^{i\phi}$. This full scattering matrix S relates the incoming edge modes to the outgoing edge modes (see, Fig. 3(a)) of the system via the relation $(b_1^\uparrow, b_1^\downarrow, b_2^\uparrow, b_2^\downarrow, b_3^\uparrow, b_3^\downarrow, b_4^\uparrow, b_4^\downarrow)^T = S(a_1^\uparrow, a_1^\downarrow, a_2^\uparrow, a_2^\downarrow, a_3^\uparrow, a_3^\downarrow, a_4^\uparrow, a_4^\downarrow)^T$. Current conservation is guaranteed by the unitarity of the scattering matrix S . The conductance matrix G of the system deduced from the full scattering matrix S , following from Eq. (1), is

$$G = \frac{e^2}{h} \frac{1}{a'} \begin{pmatrix} 2(1 - R_1 R_2 R_3 R_4) T_1 & -T_1 T_2 (R_3 R_4 + 1) & -T_1 T_3 (R_2 + R_4) & -T_1 T_4 (1 + R_2 R_3) \\ -T_1 T_2 (1 + R_3 R_4) & 2(1 - R_1 R_3 R_4) T_2 & -T_2 T_3 (R_1 R_4 + 1) & -T_2 T_4 (R_1 + R_3) \\ -T_1 T_3 (R_2 + R_4) & -T_2 T_3 (1 + R_1 R_4) & 2(1 - R_1 R_2 R_4) T_3 & -T_3 T_4 (R_1 R_2 + 1) \\ -T_1 T_4 (1 + R_3 R_2) & -T_2 T_4 (R_1 + R_3) & -T_3 T_4 (1 + R_1 R_2) & 2(1 - R_1 R_2 R_3) T_4 \end{pmatrix}, \quad (5)$$

where $a' = (1 + R_1 R_2 R_3 R_4 - 2\sqrt{R_1 R_2 R_3 R_4} \cos \phi)$. Conductance matrix G connects currents and voltages at each contact via the relation $(I_1, I_2, I_3, I_4)^T = G(V_1, V_2, V_3, V_4)^T$. Since currents through voltage probes 2 and 4 are zero, so $I_2 = I_4 = 0$, and choosing reference potential $V_3 = 0$ we get voltages V_2 and V_4 in terms of V_1 . Hall resistance $R_H^{Amp} = R_{13,24} = \frac{(V_2 - V_4)}{I_1}$, 2-terminal resistance is $R_{2T}^{Amp} = R_{13,13} = \frac{(V_1 - V_3)}{I_1}$, and non-local resistance is $R_{NL}^{Amp} = R_{12,43} = \frac{(V_4 - V_3)}{I_1}$ (to calculate the non-local resistance contacts 1,2 are used as current probes while contacts 3,4 as voltage probes). Here, we consider $D_1 = D_2 = D_u$, and $D_3 = D_4 = D_l$ for Hall resistance since for equally disordered contacts it vanishes. For 2-terminal and

Each element of the full scattering matrix S can be calculated from these S_j matrices in the following manner: an electron in a_1 edge state can scatter into b_1 edge state directly with amplitude $r_1 e^{i\phi_1}$, but then, it can also follow a different path via scattering at contacts 2,3,4 and reach b_1 edge state with amplitude: $it_1 e^{i\phi_1} \times r_2 e^{i\phi_2} \times r_3 e^{i\phi_3} \times r_4 e^{i\phi_4} \times it_1 e^{i\phi_1} = -t_1^2 r_2 r_3 r_4 e^{i(2\phi_1 + \phi_2 + \phi_3 + \phi_4)}$, and a third path with amplitude: $-t_1^2 r_1 (r_2 r_3 r_4)^2 e^{i(3\phi_1 + 2\phi_2 + 2\phi_3 + 2\phi_4)}$ and so on. Summing over all these paths we get $(1,1)^{\text{th}}$ element $s_{11}^{\uparrow\uparrow}$ of full scattering matrix S of the system, which is $(r_1 - r_2 r_3 r_4 e^{i\phi}) e^{i\phi_1} / (1 - r_1 r_2 r_3 r_4 e^{i\phi})$, with $\phi = \phi_1 + \phi_2 + \phi_3 + \phi_4$. Similarly, rest of the elements of the S matrix can be derived. The scattering matrix for 4-terminal QSH sample in Fig. 3(a) is thus:

non-local, we consider $D_u = D_l = D$. Thus,

$$R_H^{Amp} = \frac{h}{2e^2} \frac{(D_l - D_u)^2 (1 + D_l^2 D_u^2 - 2D_l D_u \cos \phi)}{(4(1 + D_l)(1 + D_u)(-1 + D_l D_u)^2 (1 + D_l D_u))},$$

$$R_{2T}^{Amp} = \frac{h}{2e^2} \frac{(1 + D^4 - 2D^2 \cos \phi)}{(1 - D^2)^2},$$

$$\text{and } R_{NL}^{Amp} = \frac{h}{2e^2} \frac{(1 + D^4 - 2D^2 \cos \phi)}{(1 + D^2)(1 + D)^2}. \quad (6)$$

The mean Hall, 2-terminal and non-local resistances obtained by averaging over the phase ϕ acquired by the electronic edge modes due to multiple scattering at disordered contacts is thus-

$$\langle R_H^{Amp} \rangle = \frac{h}{2e^2} \frac{((D_l - D_u)^2 (1 + D_l^2 D_u^2))}{(4(1 + D_l)(1 + D_u)(-1 + D_l D_u)^2 (1 + D_l D_u))},$$

$$\langle R_{2T}^{Amp} \rangle = \frac{h}{2e^2} \frac{(1 + D^4)}{(1 - D^2)^2},$$

$$\langle R_{NL}^{Amp} \rangle = \frac{h}{2e^2} \frac{(1 + D^4)}{(1 + D^2)(1 + D)^2}. \quad (7)$$

One observes that the mean Hall, 2-terminal and non-local resistances lose their quantization due to disordered contacts. To calculate the quantum localization correction, we need to calculate the resistances using probabilities ignoring the

phases acquired by edge modes at disordered contacts. The conductance matrix G is then

$$G = \frac{2e^2}{h} \frac{1}{a''} \begin{pmatrix} (1-R_2R_3R_4)T_1 & -T_1T_2R_3R_4 & -T_1T_3T_4 & -T_1T_4 \\ -T_1T_2 & (1-R_1R_3R_4)T_2 & -T_2T_3R_1R_4 & -T_2T_4R_1 \\ -T_1T_3R_2 & -T_2T_3 & (1-R_1R_2R_4)T_3 & -T_3T_4R_1R_2 \\ -T_1T_4R_3R_2 & -T_2T_4R_3 & -T_3T_4 & (1-R_1R_2R_3)T_4 \end{pmatrix}, \quad (8)$$

where $a'' = (1 - R_1R_2R_3R_4)$. As before, the current through voltage probes 2, 4 is zero, and the reference potential $V_3 = 0$. Thus, the potentials V_2 and V_4 are derived in terms of V_1 . The Hall resistance R_H , 2-terminal resistance R_{2T} , and nonlocal resistance R_{NL} calculated via probabilities are then-

$$R_H = \frac{h}{e^2} \frac{(D_u - D_l)^2}{4(1+D_l)(1+D_u)(1-D_lD_u)}, \quad R_{2T} = \frac{h}{e^2} \frac{1+D^2}{1-D^2},$$

and $R_{NL} = \frac{h}{e^2} \frac{1-D}{1+D}$. (9)

The quantum localization correction is defined as the difference in the resistances calculated from amplitudes and that from probabilities, is then $R_X^{QL} = \langle R_X^{Amp} \rangle - R_X$, with $X = H, 2T, NL$ -

$$R_H^{QL} = \frac{h}{2e^2} \frac{D_l^2 D_u^2 (D_l - D_u)^2}{2(1+D_l)(1+D_u)(1-D_l^2 D_u^2)},$$

$$R_{2T}^{QL} = \frac{h}{2e^2} \frac{2D^4}{(1-D^2)^2}, \quad R_{NL}^{QL} = \frac{h}{2e^2} \frac{D^4}{2(1+D)^2(1+D^2)} \quad (10)$$

$$S = \frac{1}{b} \begin{pmatrix} (r-r^5 e^{i\phi})e^{i\phi_1} & 0 & -t^2 r^4 e^{i\phi} & 0 & -t^2 r^3 e^{i\phi_34561} & 0 & -t^2 r^2 e^{i\phi_4561} & 0 & -t^2 r e^{i\phi_561} & 0 & -t^2 e^{i\phi_61} & 0 \\ 0 & (r-r^5 e^{i\phi})e^{i\phi_1} & 0 & -t^2 e^{i\phi_12} & 0 & -t^2 r e^{i\phi_123} & 0 & -t^2 r^2 e^{i\phi_1234} & 0 & -t^2 r^3 e^{i\phi_12345} & 0 & -t^2 r^4 e^{i\phi} \\ -t^2 r^2 e^{i\phi_12} & 0 & (r-r^5 e^{i\phi})e^{i\phi_2} & 0 & -t^2 r^4 e^{i\phi} & 0 & -t^2 r^3 e^{i\phi_45612} & 0 & -t^2 r^2 e^{i\phi_5612} & 0 & -t^2 r e^{i\phi_612} & 0 \\ 0 & -t^2 r^4 e^{i\phi} & 0 & (r-r^5 e^{i\phi})e^{i\phi_2} & 0 & -t^2 e^{i\phi_23} & 0 & -t^2 r e^{i\phi_234} & 0 & -t^2 r^2 e^{i\phi_2345} & 0 & -t^2 r^3 e^{i\phi_23456} \\ -t^2 r e^{i\phi_123} & 0 & -t^2 e^{i\phi_23} & 0 & (r-r^5 e^{i\phi})e^{i\phi_3} & 0 & -t^2 r^4 e^{i\phi} & 0 & -t^2 r^3 e^{i\phi_56123} & 0 & -t^2 r^2 e^{i\phi_6123} & 0 \\ 0 & -t^2 r^3 e^{i\phi_34561} & 0 & -t^2 r^4 e^{i\phi} & 0 & (r-r^5 e^{i\phi})e^{i\phi_3} & 0 & -t^2 r e^{i\phi_34} & 0 & -t^2 r e^{i\phi_345} & 0 & -t^2 r^2 e^{i\phi_3456} \\ -t^2 r^2 e^{i\phi_1234} & 0 & -t^2 r e^{i\phi_234} & 0 & -t^2 e^{i\phi_34} & 0 & (r-r^5 e^{i\phi})e^{i\phi_4} & 0 & -t^2 r^4 e^{i\phi} & 0 & -t^2 r^3 e^{i\phi_61234} & 0 \\ 0 & -t^2 r^2 e^{i\phi_4561} & 0 & -t^2 r^3 e^{i\phi_45612} & 0 & -t^2 r^4 e^{i\phi} & 0 & (r-r^5 e^{i\phi})e^{i\phi_4} & 0 & -t^2 e^{i\phi_45} & 0 & -t^2 r e^{i\phi_456} \\ -t^2 r^3 e^{i\phi_12345} & 0 & -t^2 r^2 e^{i\phi_2345} & 0 & -t^2 r e^{i\phi_345} & 0 & -t^2 e^{i\phi_45} & 0 & (r-r^5 e^{i\phi})e^{i\phi_5} & 0 & -t^2 r^4 e^{i\phi} & 0 \\ 0 & -t^2 e^{i\phi_561} & 0 & -t^2 r^2 e^{i\phi_5612} & 0 & -t^2 r^3 e^{i\phi_56123} & 0 & -t^2 r^4 e^{i\phi} & 0 & (r-r^5 e^{i\phi})e^{i\phi_5} & 0 & -t^2 e^{i\phi_56} \\ -t^2 r^4 e^{i\phi} & 0 & -t^2 r^3 e^{i\phi_23456} & 0 & -t^2 r^2 e^{i\phi_3456} & 0 & -t^2 r e^{i\phi_456} & 0 & -t^2 e^{i\phi_56} & 0 & (r-r^5 e^{i\phi})e^{i\phi_6} & 0 \\ 0 & -t^2 e^{i\phi_16} & 0 & -t^2 r e^{i\phi_612} & 0 & -t^2 r^2 e^{i\phi_6123} & 0 & -t^2 r^3 e^{i\phi_61234} & 0 & -t^2 r^4 e^{i\phi} & 0 & (r-r^5 e^{i\phi})e^{i\phi_6} \end{pmatrix}, \quad (11)$$

where $b = 1 - r^6 e^{i\phi}$ with $\phi_{ij..m} = \phi_i + \phi_j + \dots + \phi_m$. For simplicity, we consider all contacts to be equally disordered. r and t denote reflection and transmission amplitudes at contact i . Scattering matrix S of the 6-terminal QSH sample relates the incoming spin-polarized edge states to the outgoing states (see, Fig. 3(b)) of the system via the relation: $(b_1^\uparrow, b_1^\downarrow, b_2^\uparrow, b_2^\downarrow, b_3^\uparrow, b_3^\downarrow, b_4^\uparrow, b_4^\downarrow, b_5^\uparrow, b_5^\downarrow, b_6^\uparrow, b_6^\downarrow)^T = S(a_1^\uparrow, a_1^\downarrow, a_2^\uparrow, a_2^\downarrow, a_3^\uparrow, a_3^\downarrow, a_4^\uparrow, a_4^\downarrow, a_5^\uparrow, a_5^\downarrow, a_6^\uparrow, a_6^\downarrow)^T$. The conductance matrix \bar{G} of the sample deduced from scattering matrix

S of Eq. (11), and using Eq. (1), is

$$G = \frac{2e^2}{h} \frac{1}{b'} \begin{pmatrix} 2(1-R^5)T & -T^2 R^4 & -T^2 R^3 & -T^2 R^2 & -T^2 R & -T^2 \\ -T^2 R & 2(1-R^5)T & -T^2 R^4 & -T^2 R^3 & -T^2 R^2 & -T^2 R^2 \\ -T^2 R & -T^2 R & 2(1-R^5)T & -T^2 R^4 & -T^2 R^3 & -T^2 R^2 \\ -T^2 R^2 & -T^2 R & -T^2 R & 2(1-R^5)T & -T^2 R^4 & -T^2 R^3 \\ -T^2 R^3 & -T^2 R^2 & -T^2 R & -T^2 R & 2(1-R^5)T & -T^2 R^4 \\ -T^2 R^4 & -T^2 R^3 & -T^2 R^2 & -T^2 R & -T^2 R & 2(1-R^5)T \end{pmatrix}, \quad (12)$$

where $b' = (1 + R^6 - 2R^3 \cos \phi)$. Since current through voltage probes 2, 3, 5 and 6 is zero, so $I_2 = I_3 = I_5 = I_6 = 0$, and choosing reference potential $V_4 = 0$ we get potentials V_2, V_3, V_5 and V_6 in terms of V_1 . Thus, the Hall resistance $R_H^{Amp} = R_{14,26} = \frac{(V_2 - V_6)}{I_1}$, 2-terminal resistance $R_{2T}^{Amp} = R_{14,14} = \frac{(V_1 - V_4)}{I_1}$, longitudinal resistance $R_L^{Amp} = R_{14,23} =$

$\frac{(V_2-V_3)}{I_1}$, and non-local resistance $R_{NL}^{Amp} = R_{12,54} = \frac{(V_5-V_4)}{I_1}$ (to calculate non-local resistance, as before, contacts 1,2 are used as current probes while contacts 3,4,5,6 are voltage probes) are-

$$\begin{aligned} R_H^{Amp} &= \frac{h}{e^2} (D_u - D_l) * F, \\ &= 0 \quad (\text{when } D_l = D_u), \\ R_{2T}^{Amp} &= \frac{h}{e^2} \frac{(3 - D(2 - 3D))(1 + D^6 - 2D^3 \cos \phi)}{2(1 - D^2)^2(1 + D^2 + D^4)}, \\ R_L^{Amp} &= \frac{h}{e^2} \frac{(1 + D^6 - 2D^3 \cos \phi)}{2(1 + D)^2(1 + D^2 + D^4)}, \\ R_{NL}^{Amp} &= \frac{h}{e^2} \frac{(1 + D^6 - 2D^3 \cos \phi)}{6(1 + D)^2(1 + D^2 + D^4)}, \end{aligned}$$

where,

$$F = \frac{(1 + D_l(2 - D_u) - 2D_u)(1 + D_l^3 D_u^3 - 2\sqrt{D_l^3 D_u^3} \cos \phi)}{6(1 + D_l)(1 + D_u)(1 - D_l D_u)^2(1 + D_l D_u(1 + D_l D_u))}. \quad (13)$$

All contacts are considered to be equally disordered, i.e., $D_i = D$ (for $i = 1 - 6$). To calculate the Hall resistance only we have considered $D_1 = D_2 = D_3 = D_u$ and $D_4 = D_5 = D_6 = D_l$, otherwise for equally disordered contacts the Hall resistance is always zero. After averaging over phase shift ϕ we get,

$$\begin{aligned} \langle R_H^{Amp} \rangle &= \frac{h}{e^2} (D_u - D_l) * F', \\ &= 0, \quad (\text{when } D_l = D_u), \\ \langle R_{2T}^{Amp} \rangle &= \frac{h}{e^2} \frac{(3 - D(2 - 3D))(1 + D^6)}{2(1 - D^2)^2(1 + D^2 + D^4)}, \\ \langle R_L^{Amp} \rangle &= 3 \langle R_{NL}^{Amp} \rangle = \frac{h}{e^2} \frac{(1 + D^6)}{2(1 + D)^2(1 + D^2 + D^4)}, \end{aligned}$$

where,

$$F' = \frac{(1 + D_l(2 - D_u) - 2D_u)(1 + D_l^3 D_u^3)}{6(1 + D_l)(1 + D_u)(1 - D_l D_u)^2(1 + D_l D_u(1 + D_l D_u))}. \quad (14)$$

The quantum localization correction is the difference between the resistances calculated using probabilities, i.e., neglecting the phase acquired by the edge electrons and the resistance determined from scattering amplitudes, Eq. (13). The conductance matrix G derived from scattering probabilities is-

$$G = \frac{2e^2}{h} \frac{1}{b''} \begin{pmatrix} 2(1-R^5)T & -T^2 R^4 & -T^2 R^3 & -T^2 R^2 & -T^2 R & -T^2 \\ -T^2 & 2(1-R^5)T & -T^2 R^4 & -T^2 R^3 & -T^2 R^2 & -T^2 R \\ -T^2 R & -T^2 & 2(1-R^5)T & -T^2 R^4 & -T^2 R^3 & -T^2 R^2 \\ -T^2 R^2 & -T^2 R & -T^2 & 2(1-R^5)T & -T^2 R^4 & -T^2 R^3 \\ -T^2 R^3 & -T^2 R^2 & -T^2 R & -T^2 & 2(1-R^5)T & -T^2 R^4 \\ -T^2 R^4 & -T^2 R^3 & -T^2 R^2 & -T^2 R & -T^2 & 2(1-R^5)T \end{pmatrix}, \quad (15)$$

where $b'' = (1 - R^6)$. As before, current through voltage probes 2, 3, 5, 6 is zero, and choosing reference potential $V_4 = 0$ we get potentials V_2 and V_4 in terms of V_1 . Thus, Hall resistance R_H , 2-terminal resistance R_{2T} , longitudinal resistance

R_L , and non-local resistance R_{NL} calculated via probabilities are then-

$$\begin{aligned} R_H &= \frac{(D_u - D_l)(1 + 2D_u - D_l(2 + D_u))}{6(1 + D_l)(1 + D_u)(1 - D_l D_u)}, \\ &= 0, \quad \text{when } D_u = D_l, \\ R_{2T} &= \frac{h}{2e^2} \frac{(3 - D(2 - 3D))}{2(1 - D^2)}, \\ \text{and } R_L &= 3R_{NL} = \frac{h}{2e^2} \frac{(1 - D)}{2(1 + D)}. \end{aligned} \quad (16)$$

The quantum localization corrections to the above calculated Hall, longitudinal, 2-terminal and non-local resistances in the 6-terminal QSH sample thus are $R_X^{QL} = \langle R_X^{Amp} \rangle - R_X$, with $X = H, 2T, NL, L$ -

$$\begin{aligned} R_H^{QL} &= \frac{(D_u - D_l)(1 - D_l D_u + 2D_l^4 D_u^3 - 2D_l^3 D_u^4)}{3(1 + D_l)(1 + D_u)(1 - D_l D_u)^2(1 + D_l D_u + D_l^2 D_u^2)} \\ &= 0, \quad \text{when } D_u = D_l, \\ R_{2T}^{QL} &= \frac{h}{2e^2} \frac{D^6(3 - 2D + 3D^2)}{(1 - D^2)^2(1 + D^2 + D^4)}, \\ \text{and } R_L^{QL} &= 3R_{NL}^{QL} = \frac{h}{2e^2} \frac{D^6}{(1 + D)^2(1 + D^2 + D^4)}. \end{aligned} \quad (17)$$

From Eq. (17) we see that the quantum localization correction for Hall resistance in a six terminal QSH sample can be positive as well as negative depending on the strength of disorder at different contacts while for four terminal QSH sample it is always positive, see Eq. (10). This negative correction term does not imply anti-localization of the helical electrons, rather it comes from the fact that the Hall resistance for QSH sample itself can be negative. However, the absolute value of resistances calculated via amplitudes is always greater than the absolute value of the resistances derived via probabilities, i.e., $|\langle R_H^{Amp} \rangle| > |R_H|$. This negative quantum localization correction for Hall resistance is unique to QSH samples only and not present for QH samples, see Ref. [9]. From Eq. (17) it can also be noted that for equally disordered contacts the quantum localization correction for Hall resistance vanishes for QSH samples while for QH samples it is finite, see Ref. [9]. The quantum localization correction to the 2-terminal, longitudinal and non-local resistances increases with increasing disorder while the same for Hall resistance increases with the increase of the difference between the disorderedness of upper (D_u) and lower (D_l) contacts.

V. N TERMINAL SYSTEM WITH ALL CONTACTS DISORDERED

An N-terminal QSH sample is shown in Fig. 3(c) with all contacts equally disordered, i.e., $D_1 = D_2 = \dots = D_N = D$. Contacts 1 and k are current probes and contacts 2, 3, ..., $k-1, k+1, \dots, N$ are voltage probes, thus current through these contacts, i.e., $I_2 = I_3 = \dots = I_{k-1} = I_{k+1} = \dots = I_N = 0$. The scattering matrix for the N-terminal QSH sample in Fig. 3(c) is

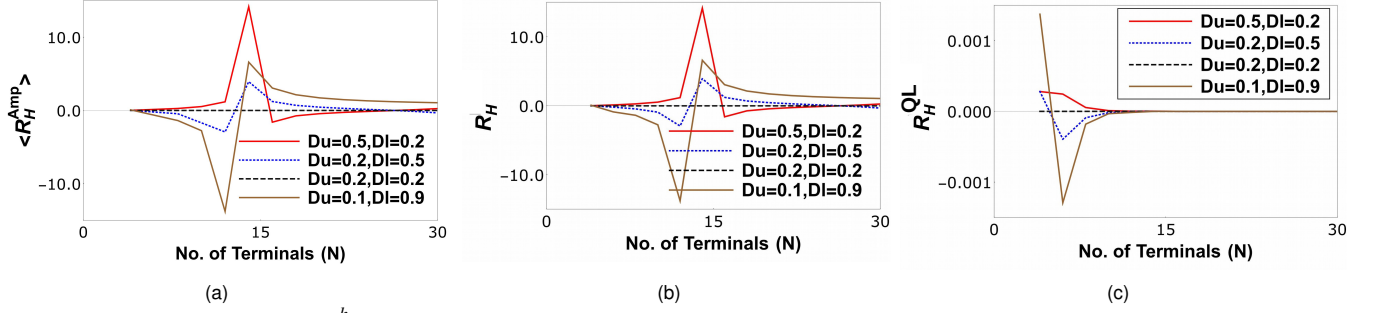


Figure 4. Hall resistance in units of $\frac{h}{e^2}$ calculated (a) via scattering amplitudes and (b) via probabilities for a N terminal QSH sample with lower edge contacts disordered with strength D_l and upper edge contacts disordered with strength D_u , (c) the quantum localization correction to the Hall resistance.

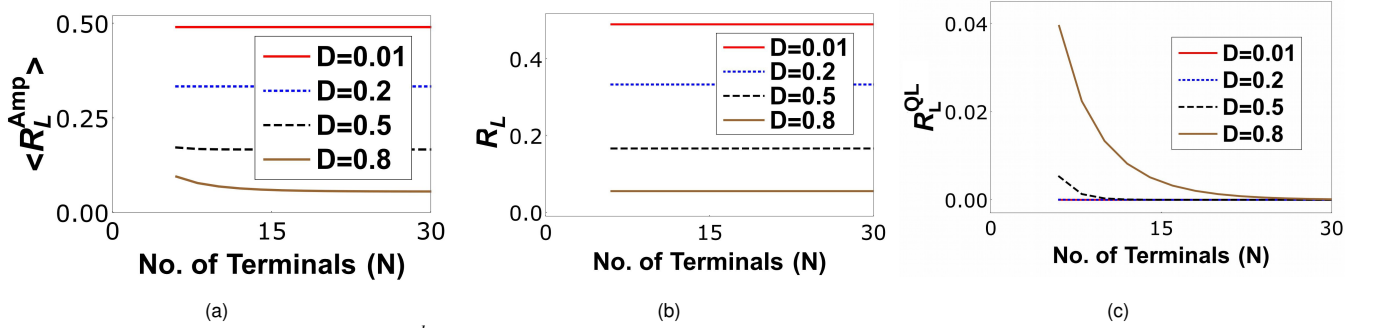


Figure 5. Longitudinal resistance in units of $\frac{h}{e^2}$ calculated (a) via scattering amplitudes, and (b) via probabilities for an N-terminal QSH sample with all contacts equally disordered, and (c) the quantum localization correction to the longitudinal resistance.

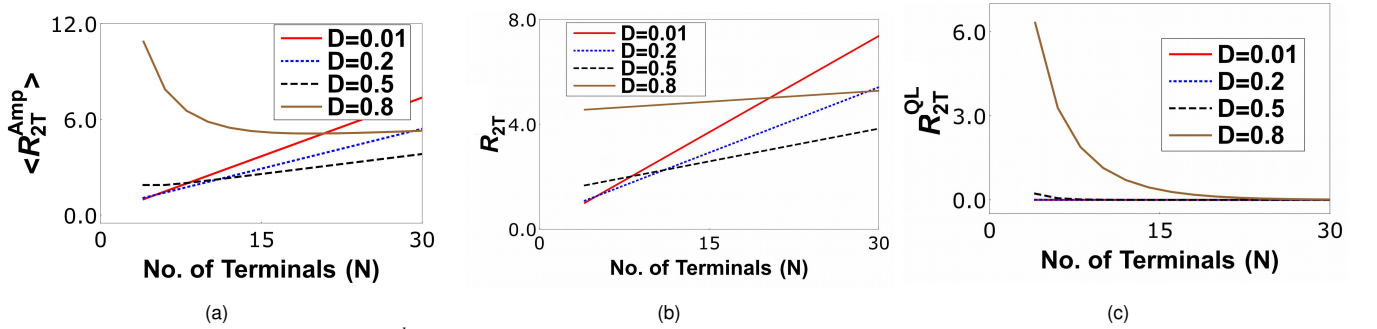


Figure 6. 2-terminal resistance in units of $\frac{h}{e^2}$ calculated (a) via scattering amplitudes, (b) via probabilities for a N-terminal QSH sample with all contacts equally disordered, and (c) the quantum localization correction to the 2T resistance.

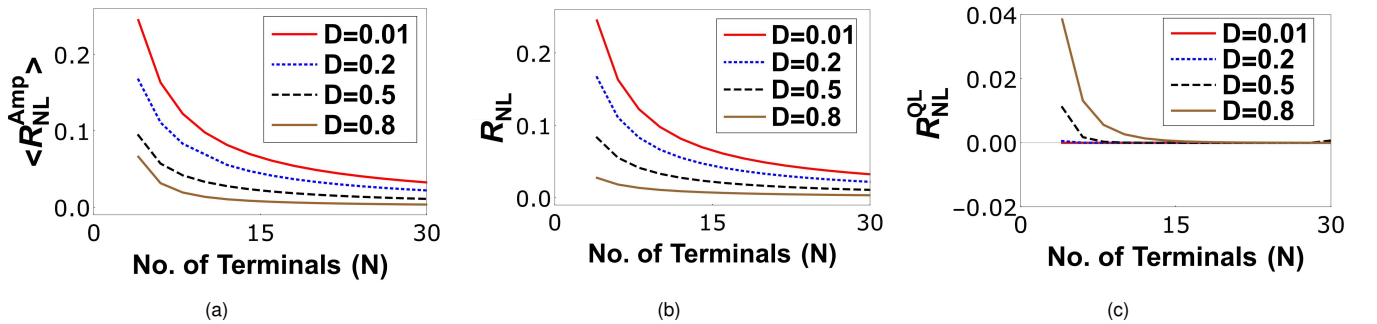


Figure 7. Non-local resistance in units of $\frac{h}{e^2}$ calculated (a) via scattering amplitudes, (b) via probabilities for a N-terminal QSH sample with all contacts equally disordered, and (c) the quantum localization correction to the non-local resistance.

$$S = \frac{1}{c} \begin{pmatrix} (r-r^{N-1}e^{i\phi})e^{i\phi_1} & 0 & \dots & -t^2r^{N-k}e^{i\phi_{k(k+1)..1}} & 0 & \dots & -t^2e^{i\phi_{N1}} & 0 \\ 0 & (r-r^{N-1}e^{i\phi})e^{i\phi_1} & \dots & 0 & -t^2r^{k-2}e^{i\phi_{12..k}} & \dots & 0 & -t^2r^{N-2}e^{i\phi_{12..N}} \\ \vdots & \vdots & \dots & \vdots & \vdots & \dots & \vdots & \vdots \\ -t^2r^{k-2}e^{i\phi_{12..k}} & 0 & \dots & (r-r^{N-1}e^{i\phi})e^{i\phi_k} & 0 & \dots & -t^2r^{k-1}e^{i\phi_{N12..k}} & 0 \\ 0 & -t^2r^{N-k}e^{i\phi_{k(k+1)..1}} & \dots & 0 & (r-r^{N-1}e^{i\phi})e^{i\phi_k} & \dots & 0 & -t^2r^{N-k-1}e^{i\phi_{k(k+1)..N}} \\ \vdots & \vdots & \dots & \vdots & \vdots & \dots & \vdots & \vdots \\ -t^2r^{N-2}e^{i\phi_{12..N}} & 0 & \dots & -t^2r^{N-k-1}e^{i\phi_{k(k+1)..N}} & 0 & \dots & (r-r^{N-1}e^{i\phi})e^{i\phi_N} & 0 \\ 0 & -t^2e^{i\phi_{N1}} & \dots & 0 & -t^2r^{k-1}e^{i\phi_{N12..k}} & \dots & 0 & (r-r^{N-1}e^{i\phi})e^{i\phi_N} \end{pmatrix}, \quad (18)$$

where $c = 1 - r^N e^{i\phi}$ and $\phi_{ij..k} = \phi_i + \phi_j + \dots + \phi_k$. The scattering matrix connects the incoming edge states to the outgoing edge states via the relation $(b_1^\uparrow, b_1^\downarrow, \dots, b_k^\uparrow, b_k^\downarrow, \dots, b_N^\uparrow, b_N^\downarrow)^T = S(a_1^\uparrow, a_1^\downarrow, \dots, a_k^\uparrow, a_k^\downarrow, \dots, a_N^\uparrow, a_N^\downarrow)$. The conductance matrix G of the N -terminal QSH sample derived from the scattering matrix S , following Eq. (1), is thus-

$$G = \frac{1}{c'} \begin{pmatrix} 2T(1-R^{N-1}) & \dots & -T^2(R^{N-k}+R^{k-2}) & \dots & -T^2(1+R^{N-2}) \\ -T^2(R^{k-2}+R^{N-k}) & \dots & 2T(1-R^{N-1}) & \dots & -T^2(R^{k-1}+R^{N-k-1}) \\ \vdots & \vdots & \vdots & \vdots & \vdots \\ -T^2(R^{N-2}+1) & \dots & -T^2(R^{N-k-1}+R^{k-1}) & \dots & 2T(1-R^{N-1}) \end{pmatrix}, \quad (19)$$

where $c' = 1 + R^N - 2R^{N/2} \cos \phi$. Since currents through voltage probes $2, 3, \dots, k-1, k+1, \dots, N$ is zero, so $I_2 = I_3 = \dots = I_{k-1} = I_{k+1} = I_N = 0$, and choosing reference potential $V_k = 0$ we get potentials $V_2, V_3, V_{k-1}, V_{k+1}$ and V_N in terms of V_1 . So, Hall resistance $R_H^{Amp} = R_{1k,2N} = \frac{(V_2 - V_N)}{I_1}$, 2-terminal resistance $R_{2T}^{Amp} = R_{1k,1k} = \frac{(V_1 - V_k)}{I_1}$, longitudinal resistance $R_L^{Amp} = R_{1k,23} = \frac{(V_2 - V_3)}{I_1}$ and non-local resistance $R_{NL}^{Amp} = R_{12,(k+1)k} = \frac{(V_{k+1} - V_k)}{I_1}$. To calculate non-local resistance we consider contacts 1,2 as current probes and contacts 3,4, ..., $k-1, k, k+1, \dots, N$ as voltage probe. As the expressions for these resistances are large, we analyze them via plots, see Figs. (4-7). The average resistances for N -terminal case are found by averaging over the phases. Thus $\langle R_X^{Amp} \rangle = \frac{1}{2\pi} \int_0^{2\pi} R_X d\phi$. To calculate the quantum localization correction, we need to calculate the conductance using probabilities ignoring the phase acquired by the edge electrons. The conductance matrix G derived via transmission probabilities is then

$$G = \frac{1}{c''} \begin{pmatrix} 2T(1-R^{N-1}) & \dots & -T^2(R^{N-k}+R^{k-2}) & \dots & -T^2(1+R^{N-2}) \\ -T^2(R^{k-2}+R^{N-k}) & \dots & 2T(1-R^{N-1}) & \dots & -T^2(R^{k-1}+R^{N-k-1}) \\ \vdots & \vdots & \vdots & \vdots & \vdots \\ -T^2(R^{N-2}+1) & \dots & -T^2(R^{N-k-1}+R^{k-1}) & \dots & 2T(1-R^{N-1}) \end{pmatrix} \quad (20)$$

where $c'' = (1 - R^N)$. Setting the current, as before, through voltage probes $2, 3, \dots, k-1, k+1, \dots, N$ to zero, and choosing reference potential $V_k = 0$ we get potentials $V_2, V_3, V_{k-1}, V_{k+1}$ and V_N in terms of V_1 . Similarly, we need to calculate the Hall resistance R_H , 2-terminal resistance R_{2T} , and nonlocal resistance R_{NL} via probabilities from the conductance matrix as in Eq. (20). As these expressions are large, we analyze them in Figs. (4-7). The quantum localization correction, as defined before, is $R_X^{QL} = \langle R_X^{Amp} \rangle - R_X$ with $X = H, 2T, L, NL$. One can get a closed form expression for a general N (with $N = \text{even}$)-terminal system as well by looking at the 6, 8, 10... terminal resistances. This is written below for the quantum lo-

calization correction, resistance derived via probabilities and that derived from amplitudes in case of longitudinal and non-local resistances-

$$\begin{aligned} R_L^{Amp} &= \frac{N}{2} R_{NL}^{Amp} = \frac{h}{2e^2} \frac{1 + D^N - 2D^{N/2} \cos \phi}{(1+D)^2 2(1+D^2+D^4+\dots+D^{N-2})}, \\ \langle R_L^{Amp} \rangle &= \frac{N}{2} \langle R_{NL}^{Amp} \rangle = \frac{h}{2e^2} \frac{1 + D^N}{(1+D)^2 2(1+D^2+D^4+\dots+D^{N-2})}, \\ R_L &= \frac{N}{2} R_{NL} = \frac{h}{2e^2} \frac{(1-D)}{2(1+D)}, \\ R_L^{QL} &= \frac{N}{2} R_{NL}^{QL} = \frac{h}{2e^2} \frac{D^N}{(1+D)^2 (1+D^2+D^4+\dots+D^{N-2})}. \end{aligned} \quad (21)$$

For simplicity, we consider in Eq. (21) all contacts to be equally disordered. No closed form expression can be systematically deduced for Hall and 2-terminal cases as there is no uniformity in going from 6, 8, 10 terminal and likewise cases. In Figs. (4-7) we analyze the quantum localization correction for various resistances. In Figs. 4(a,b), we see that Hall resistance for QSH case can be either negative or positive depending on disorder strength at upper edge (D_u) and lower edge (D_l) contacts. If $D_u = D_l$, then Hall resistance is zero in case of calculation using scattering amplitudes or probabilities. In Fig. 4(c) we see that the quantum localization correction to the Hall resistance can also be negative, which again does not imply that it leads to anti-localization. The Hall resistance for QSH itself can be negative, and that leads to a negative localization correction term, although $|\langle R_H^{Amp} \rangle| > |R_H|$. The longitudinal resistance is almost constant as function of the number of contacts. However, the stronger the disorderedness of contacts the lower the longitudinal resistance. In Fig. 5(c), we see that the quantum localization correction decreases with increase in number of contacts unlike in quantum Hall samples where it is always zero, see Ref. [9]. In Fig. 6(a,b) we see that the 2-terminal resistance for QSH case increases with number of contacts (unlike the QH case), which implies the 2-terminal resistance increases as a function of the length of the sample. This is similar to what is observed for Ohmic behavior. In Fig. 6(c) we see that the quantum localization correction is very small for $D < 1/2$, only for $D > 1/2$ it becomes substantial. In Figs. 4-7 we see that for large number of terminals the quantum localization correction disappears. Quantum localization correction is substantial only for strong disorder and few terminals.

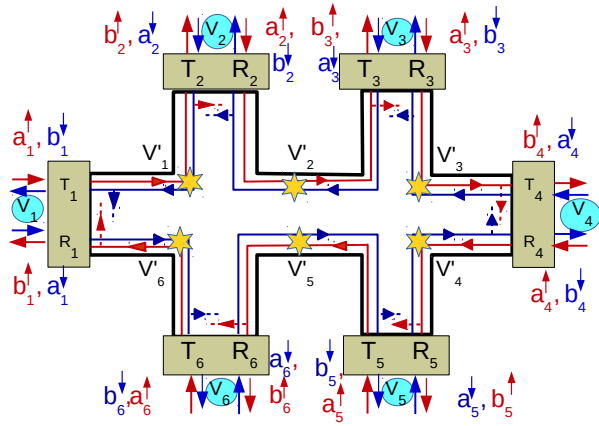


Figure 8. 6 terminal QSH bar with all disordered contacts and inelastic scattering.

VI. EFFECT OF INELASTIC SCATTERING ON QUANTUM LOCALIZATION CORRECTION

A 6-terminal QSH sample with all disordered contacts and with inelastic scattering is shown in Fig. 8. When the length between the disordered contacts is larger than the phase coherence length for electronic edge modes, inelastic scattering occurs. In presence of inelastic scattering spin up edge electrons coming out of contact 1 equilibrate with other spin up and down electrons at equilibrating potential V'_1 and lose their phase acquired via scattering at the contacts via equilibration of their energy. Similarly spin down electrons coming out of contact 1 lose their phase at equilibrating potential V'_6 via equilibration of their energies with other spin up and down electrons. Thus, there is no possibility for an electron in a edge state to get back to the same contact after emerging out of it at that energy and with a unique phase. Thus, there is no difference between resistances calculated via probabilities and that via amplitudes. This implies absence of quantum localization correction in presence of inelastic scattering. Using probabilities the resistances have already been derived, see Refs. [16, 17], as-

$$R_H = 0, \quad R_{2T} = \frac{h}{e^2} \frac{(3-D)}{(1-D^2)}, \quad R_L = 3R_{NL} = \frac{h}{e^2} \frac{1}{(1+D)}, \quad (22)$$

with $R_X = \langle R_X^{Amp} \rangle$, $X = H, L, 2T, NL$. Here, we have only concentrated on the six terminal QSH system, as in 4- and N-terminal QSH sample we obtain exactly similar results wherein inelastic scattering completely kills the quantum localization correction.

Table1: Comparison of the quantum localization correction in 6-terminal QH [9] and QSH sample with equally disordered contacts

	Quantum Hall	Quantum spin Hall
R_H^{QL}	$\frac{h}{2e^2} \frac{2D^6}{1-D^6}$	0
R_L^{QL}	0	$\frac{h}{2e^2} \frac{D^6}{(1+D)^2(1+D^2+D^4)}$
R_{2T}^{QL}	$\frac{h}{2e^2} \frac{2D^6(1+D)}{(1-D)(1-D^6)}$	$\frac{h}{2e^2} \frac{D^6(3-2D+3D^2)}{(1-D^2)^2(1+D^2+D^4)}$
R_{NL}^{QL}	0	$\frac{h}{2e^2} \frac{D^6}{3(1+D)^2(1+D^2+D^4)}$

VII. CONCLUSION

We see that resistances are affected by the quantum localization correction but only when all contacts are disordered. The quantum localization correction for the resistances for both QH (see Ref. [9]) and QSH six terminal samples are summarized and compared in Table 1. From Table 1, we see that for equally disordered contacts in QH sample only 2-terminal and Hall resistances are affected by the quantum localization correction, while in QSH sample the 2-terminal, longitudinal and non-local resistances are affected by the same correction. Quantum localization correction term arises in a QSH or QH sample due to multiple paths available edge mode electrons due to the fact that all contacts are disordered as explained in section II. However, summing the multiple paths available for helical edge modes in QSH samples and chiral edge modes in QH sample leads to a difference in the quantum localization correction. A remark on the table- the vanishing quantum localization correction doesn't mean $\langle R_{L,NL}^{Amp} \rangle = R_{L,NL}$ for a QH sample or $\langle R_H^{Amp} \rangle = R_H$ for a QSH sample but rather because $\langle R_{L,NL}^{Amp} \rangle = R_{L,NL} = 0$ for QH sample and same for Hall resistance in QSH sample. This suggests that the quantum localization correction term is finite only when resistances calculated via scattering amplitudes or probabilities are themselves finite.

In QSH samples we even see a negative localization correction, which is not due to the anti localization of the states, but rather due to the fact that the Hall resistance in a QSH system can itself turn negative. In presence of inelastic scattering this quantum localization term vanishes for both QH and QSH cases. In this letter, we have assumed disorder only at the contacts, there is no disorder within the sample. Generally, edge modes in QH/QSH samples suffer some amount of scattering at contacts. The presence of disorder within the sample wont affect the results of our letter, since it is well known that QH and QSH edge modes are robust to sample disorder. Disorder at contacts works as a barrier to edge mode transport, edge modes can partially transmit into the contacts through the barrier with probability T or can be partially reflected with probability R . In case one has completely clean contacts, one can design sample contacts to partially reflect edge modes at contacts by directly doping non-magnetic impurities or via creating an electrostatic barrier at the contacts. In Refs. [21, 22], the authors have studied sample disorder in quantum Hall systems via doping impurities within the sample. Similarly, impurities can be doped into contacts in a QSH sample thus realizing our setups and verifying the quantum localization correction.

ACKNOWLEDGMENTS

This work was supported by funds from SERB, Dept. of Science and Technology, Government of India, Grant No. EMR/2015/001836.

-
- [1] J. Asboth, L. Oroszlany and A. Palyi, A Short Course on Topological Insulators: Band-structure topology and edge states in one and two dimensions, Lecture Notes in Physics, 919 (2016).
- [2] J. Maciejko, T. L. Hughes and S-C Zhang, The Quantum Spin Hall Effect, *Annu. Rev. Condens. Matter Phys.* 2, 31-53 (2011).
- [3] M. Z. Hasan, and C. L. Kane, Colloquium: Topological insulators, *Rev. Mod. Phys.* 82, 3045 (2010).
- [4] B. L. Al'tshuler, and P. A. Lee, Disordered electronic systems. *Physics Today*, 41, 36-45 (1988).
- [5] S. Datta, Electronic transport in Mesoscopic systems (chapter 5), (Cambridge University Press, Cambridge, England, 1995).
- [6] A. Narayan and S. Sanvito, Multiprobe Quantum Spin Hall Bars, *Eur. Phys. J. B* 87: 43 (2014).
- [7] A. P. Protogenov, V. A. Verbus and E. V. Chulkov, Nonlocal Edge State Transport in Topological Insulators, *Phys. Rev. B* 88, 195431 (2013).
- [8] M. Buttiker, Absence of Backscattering in The Quantum Hall effect in Multiprobe Conductors, *Phys. Rev. B* 38, 9375 (1988); M. Buttiker, *Surface Science* 229, 201 (1990).
- [9] Arjun Mani and Colin Benjamin, Quantum localization correction to chiral edge mode transport, arXiv:1812.11799 (2018).
- [10] J. I. Vayrynen, et. al., Noise-Induced Backscattering in a Quantum Spin Hall Edge, *Phys. Rev. Lett.* 121, 106601 (2018).
- [11] C-H Hsu, et. al., Nuclear-spin-induced localization of edge states in two-dimensional topological insulators, *Phys. Rev. B* 96, 081405(R) (2017).
- [12] J. Li, R-L Chu, J. K. Jain and S-Q Shen, Topological Anderson Insulator, *Phys. Rev. Lett.* 102, 136806 (2009).
- [13] P. Delplace, J. Li and M. Buttiker, Magnetic-Field-Induced Localization in 2D Topological Insulators, *Phys. Rev. Lett.* 109, 246803 (2012).
- [14] P. Sternativo and F. Dolcini, Effects of disorder on electron tunneling through helical edge states, *Phys. Rev. B* 90, 125135 (2014).
- [15] M. Buttiker, Edge-State Physics Without Magnetic Fields, *Science* 325, 278 (2009).
- [16] A. Mani, C. Benjamin, Fragility of non-local edge mode transport in the quantum spin Hall state, *Phys. Rev. Applied.* 6, 014003 (2016).
- [17] A. Mani, C. Benjamin, Are quantum spin Hall edge modes more resilient to disorder, sample geometry and inelastic scattering than quantum Hall edge modes?, *J. Phys.: Condens. Matter* 28 (2016) 145303.
- [18] A. Mani, C. Benjamin, Probing helicity and the topological origins of helicity via non-local Hanbury-Brown and Twiss correlations, *Scientific Reports* 7: 6954 (2017).
- [19] A. Roth, et. al., Nonlocal Transport in the Quantum Spin Hall State, *Science* 325, 294 (2009); C Brune et. al., *Nature Physics*, 8, 485-490 (2012).
- [20] Y. Imry, Introduction to mesoscopic physics, 2nd edition, Oxford University Press (2001).
- [21] John D. Watson, Growth of low disorder GaAs/AlGaAs heterostructures by molecular beam epitaxy for the study of correlated electron phases in two dimensions, Ph. D thesis Purdue Univ. (2015), available at https://docs.lib.purdue.edu/open_access_dissertations/585.
- [22] Wanli Li, Scaling and Universality of Integer Quantum Hall Plateau-to-Plateau Transitions, *Phys. Rev. Lett.* 94, 206807 (2005).